ICAS 2016
30th Congress of the International Council of the Aeronautical Sciences
DCC, Daejeon, Korea ; September 25-30, 2016

ADAPTIVE NEURAL NETWORK CONTROLLER DESIGN FOR BLENDED-WING UAV WITH COMPLEX DAMAGE

Kijoon Kim*, Jongmin Ahn, Seungkeun Kim*, Jinyoung Suk***
***Chungnam National University, **Agency for Defense and Development**

Keywords: *Neural network Controller, Blended wing body, Complex damage*

Abstract

This paper presents neural network controller design for complex damage to a blended wing UAV (Unmanned Aerial Vehicle): partial loss of main wing and vertical tail. Longitudinal/lateral axis instability and the change of flight dynamics is investigated via numerical simulation. Based on this, neural network based adaptive controller combined with feedback linearization is designed in order to compensate for the complex damage. Numerical simulation verifies that the instability from the complex damage of the UAV can be stabilized via the proposed adaptive controller.

1 Introduction

Modern UAVs require high survivability and high reliability during the mission. Recently, research of reconfigurable control system for survivability has been widely performed [1, 2]. Dydek et.al carried out the design of the MRAC (Model Reference Adaptive Control), followed by a comparison of flight test results using the existing linear and augmented adaptive controllers for the quadrotor UAVs [3]. And Chowdhary et.al presents control algorithms for guidance and control of airplanes under actuator failures and severe structural damage [4].

This paper considers a complex damaged blended-wing UAV. Damaged location is main wing and vertical tail. Numerical modelling of the UAV is based on wind tunnel test. Here, each damage location causes the multi-axis instability. The neural network controller is designed to remove the abrupt motion caused by complex damage. The organization of the paper is as follows. Section 2 discusses the shape and numerical model of a blended wing body UAV considering the complex damages. Section 3 deals with linear dynamic inversion and neural network controller structure and design. Then, Section 4 shows numerical simulation results. Finally, conclusions is given in Section 5.

2 UAV numerical model

A blended-wing body type UAV is considered for this study, and partial loss of right wing and vertical tail is considered as the aircraft's damage [5]: in detail, 22% loss of area moment of the right main wing and 25% loss of effectiveness of the vertical tail. Fig. 1 shows the geometry of the blended-wing body type UAV considered in this research, whose body/span lengths and mass are 1.85 m/2 m and 12 kilograms, respectively.

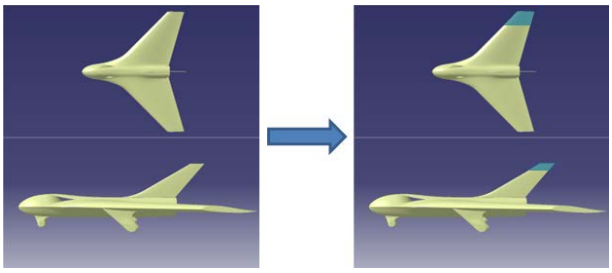

Fig. 1 Damage Configuration of the Blended Wing Body UAV.

The following force and moment equations are used for the damaged asymmetric aircraft.

$$F_B = m\frac{dv}{dt} + m\frac{d\omega}{dt}\times\Delta r + m\omega\times\frac{d\Delta r}{dt} - W \quad (1),$$

$$M_B = I\frac{d\omega}{dt} + m\Delta r\times\frac{dv}{dt} + \omega\times I\omega + m\omega\times(\Delta r\times v) \quad (2),$$

where v is velocity vector, ω is angular velocity, W is $mg[-sin\theta\ \ cos\theta sin\phi\ \ cos\theta cos\phi]^T$, Δr is the change of the C.G. location and m denotes the mass of the damaged aircraft.

Table 1 Parameter Change due to Damage.

Parameter	Change Contents
Mass	$m' = m_0 - \Delta m$
C.G.	$r' = r_0 + \Delta r$
M.O.I.	$I_{xy}, I_{yz} \neq 0$
Aerodynamic coef.	$C'_{(\,)} = C_{(\,)} - \Delta C_{(\,)}$

*x': Damaged; x0: No Damaged; Δx: Variation

3 Controller design

3.1 Inversion controller

This section presents a neural network adaptive controller design combined with feedback linearization. Figure 2 shows the general neural network controller structure.

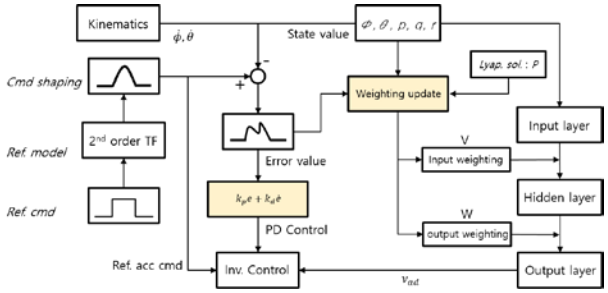

Fig. 2 Neural Network Controller Structure.

Consider a nonlinear system as

$$\dot{x}_1 = x_2 \quad (3),$$
$$\dot{x}_2 = f(x,u) \quad (4),$$

where x_1, x_2 represent state vectors of roll angle and roll angular rate, pitch angle and pitch angular rate. Eq.(4) is rephrased with the known dynamics $\hat{f}$ and un known part Δ as :

$$\dot{x}_2 = \hat{f}(x,u) + \Delta(x,u) \quad (5).$$

Recasting the known part $\hat{f}(x,u)$ to a pseudo control ν gives

$$\dot{x}_2 = \nu + \Delta \quad (6).$$

The pseudo control is designed with the linear control signal ν_c and the adaptive signal ν_{ad} as:

$$\nu = \dot{x}_{2d} + \nu_c - \nu_{ad} \quad (7).$$

Let the linear control ν_c be a PD controller.

$$\ddot{x} = \ddot{x}_d + k_{dx}\dot{e}_x + k_{px}e_x - \nu_{adx} + \Delta_x \quad (8),$$
$$\ddot{e}_x + k_{dx}\dot{e}_x + k_{px}e_x = \nu_{adx} - \Delta_x \quad (9).$$

The closed-loop system can be expressed by a matrix form as:

$$\dot{\bar{e}}_x = A_x\bar{e}_x + B_x(\nu_{adx} - \Delta_x) \quad (10),$$

where

$$A_x = \begin{bmatrix} 0 & 1 \\ -k_{px} & -k_{dx} \end{bmatrix} \quad (11),$$
$$B_x = \begin{bmatrix} 0 \\ 1 \end{bmatrix} \quad (12).$$

Substituting A_x and B_x for Eq.(10), gives Eq.(13).

$$\begin{bmatrix} \dot{e}_x \\ \ddot{e}_x \end{bmatrix} = \begin{bmatrix} 0 & 1 \\ -k_{px} & -k_{dx} \end{bmatrix} \begin{bmatrix} e_x \\ \dot{e}_x \end{bmatrix} + \begin{bmatrix} 0 \\ 1 \end{bmatrix} (\nu_{adx} - \Delta_x) \quad (13).$$

Where both k_p and k_d are real positive values. With the above form, A_x is Hurwitz. If the neural network controller is to remove the model uncertainty, then system will be stable. The original control input is represented as:

$$u = \hat{f}^{-1}(x,\nu) \quad (14).$$

3.2 Neural network adaptive controller

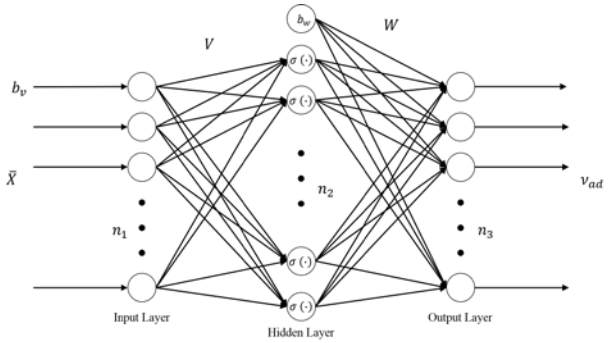

Fig. 3 Structure of a Neural Network with a Single Hidden Layer.

Fig. 3 shows the structure of a neural network with a single hidden layer. The modeling uncertainty, Δ, is a function of states that should be used as input variables to the neural network with a bias term b_v. The inversion dynamics can be obtained from neural network with a single hidden layer. Input variable to the neural network is as follows.

$$\bar{x} = [1\ v_t\ p\ q\ r\ \phi\ \theta\ \psi] \quad (15).$$

In the hidden layer, the weighted input variable z is activated by a sigmoid activation function, $\sigma(z)$:

$$\sigma(z) = \frac{1}{1+e^{-az}} \quad (16),$$
$$z = V^T\bar{x} \quad (17),$$

where a is an activation potential gain.

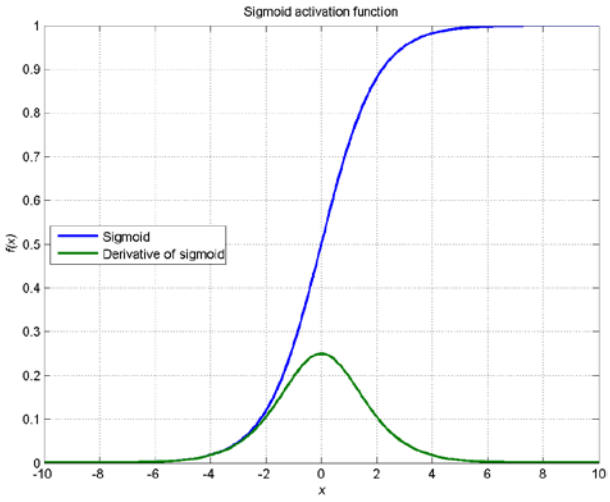

Fig. 4 Sigmoid activation function

The update law of the neural network weights is designed as [6]

$$\dot{V} = -(2\bar{x}e^T PBW^T\sigma_z + \lambda V)\Gamma_V \quad (18),$$
$$\dot{W} = -[2(\sigma - \sigma_z V^T\bar{x})e^T PB + \lambda W]\Gamma_W \quad (19),$$

where P is the positive definite solution to the Lyapunov equation:

$$A^T P + PA + Q = 0 \quad (20).$$

3.3 Inversion controller structure

This paper proposes the two types of inversion controller structures. First one is designed to separate the longitudinal and lateral axis. Second one is designed as the longitudinal and lateral axis. First inversion controller an integrate form between generates the separated elevator and aileron deflections as follows.

$$\delta_e = (\nu_\theta - M_q q)/M_{\delta_e} \quad (21)$$
$$\delta_a = (\nu_\phi - L_p p)/L_{\delta_a} \quad (22)$$

Second inversion controller generates the integrate control surface command of each axis.

$$\begin{bmatrix}\delta_e \\ \delta_a\end{bmatrix} = \begin{bmatrix}M_{\delta_e} & M_{\delta_a} \\ L_{\delta_e} & L_{\delta_a}\end{bmatrix}^{-1}\left(\begin{bmatrix}\nu_\theta \\ \nu_\phi\end{bmatrix} - \begin{bmatrix}M_q & M_p \\ L_q & L_p\end{bmatrix}\begin{bmatrix}q \\ p\end{bmatrix}\right) \quad (23).$$

4 Numerical simulation

The complex damage occurs at one second in the simulation. Immediately after the damage, roll angle experiences abrupt change. Despite of the serious situation, the neural network controller completely recovers the UAV to the original trim state. Also control surface moves to a new trim condition. Then, an individual doublet command input for roll and pitch is given as $\pm$2.5deg for total 3 seconds, respectively as shown in Figure 5.

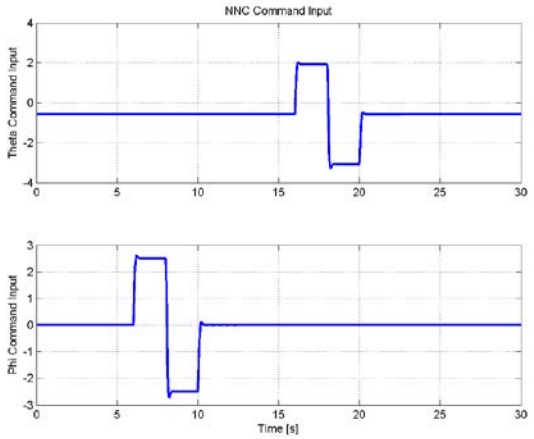

Fig. 5 Reference command inputs

4.1 No damage condition simulations

This simulation considers normal condition without damage for basic performance evaluation.

4.1.1 Case 1 (Separated pitch/roll control)

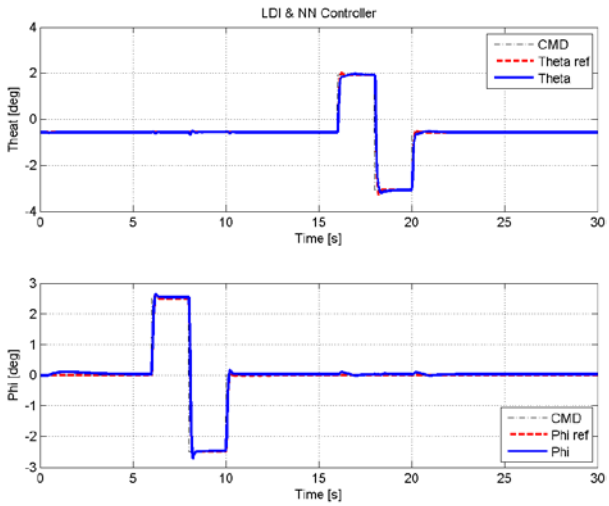

Fig. 6 Responses of state (Top: Pitch angle, Bottom: Roll angle)

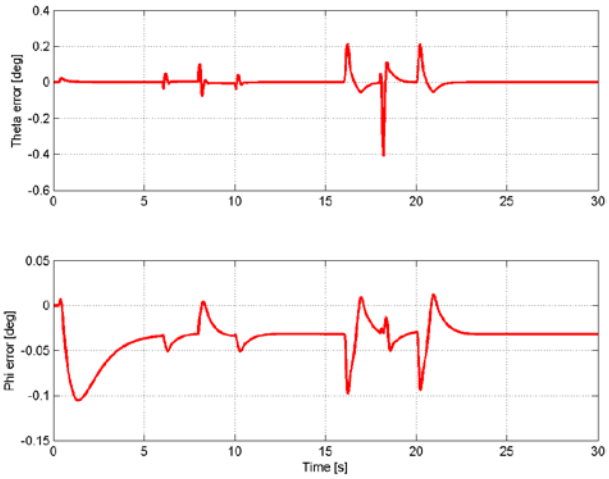

Fig. 7 Attitude error (Top: Pitch angle, Bottom: Roll angle)

4.1.2 Case 2 (Integrated pitch/roll control)

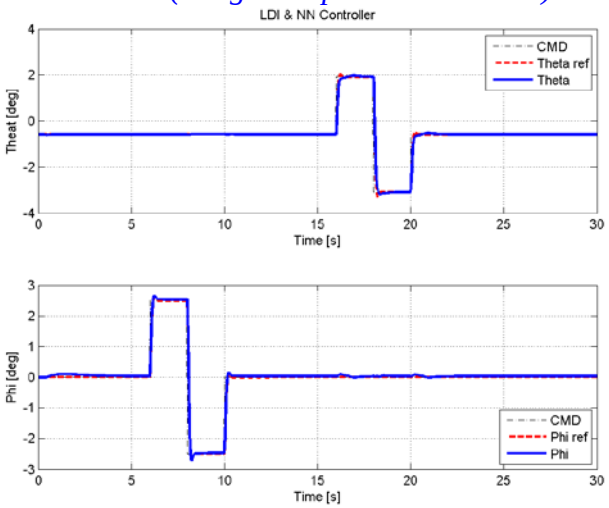

Fig. 8 Responses of state (Top: Pitch angle, Bottom: Roll angle)

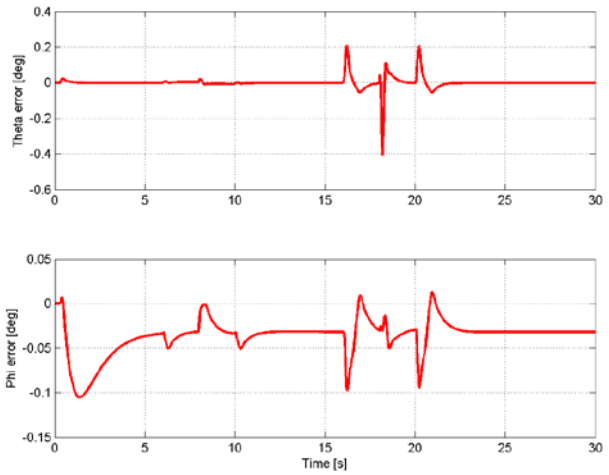

Fig. 9 Attitude error (Top: Pitch angle, Bottom: Roll angle)

Both cases show good command tracking performance, and similar responses.

4.2 Complex damage condition simulations

This simulation considers complex damage UAVs main wing and vertical tail.

4.2.1 Case 1 (Separated pitch/roll control)

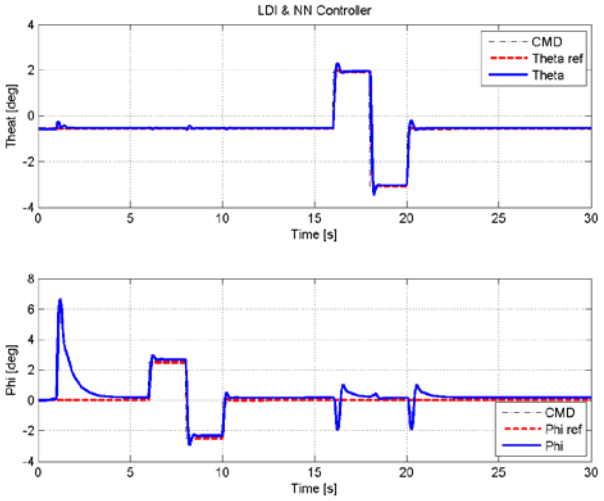

Fig. 10 Responses of state (Top: Pitch angle, Bottom: Roll angle)

Figure 10 shows the pitch and roll axis responses. Complex damage occurs in one second in the simulation. The roll and pitch axis coupling take effect near 15 seconds caused by damage.

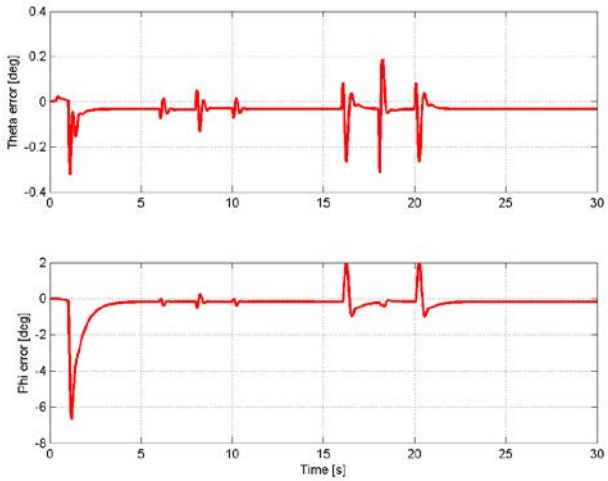

Fig. 11 Attitude error (Top: Pitch angle, Bottom: Roll angle)

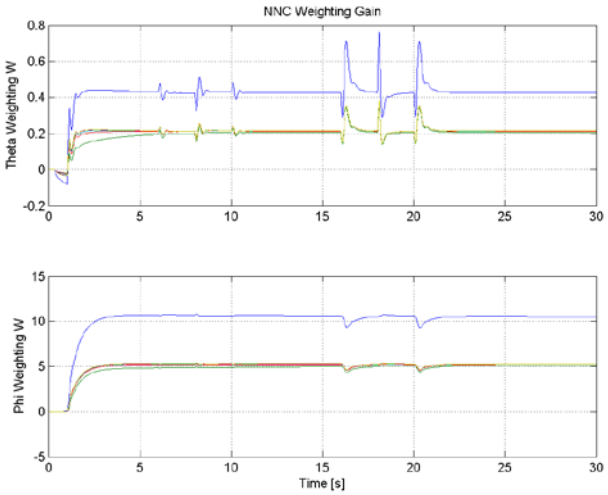

Fig. 12 NN adaptation weight W (Top: Pitch angle, Bottom: Roll angle)

Figure 11 shows the error of each axis. The roll axis error appears significantly caused by the main wing damage. Also, roll axis output layer gain is remarkably larger than pitch axis gain.

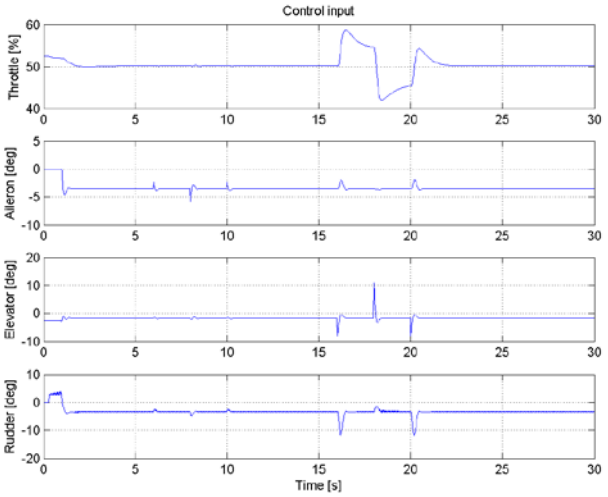

Fig. 13 Responses of throttle and control surfaces

Each axis control surface and throttle control input shows reasonable motions.

4.2.1 Case 2 (Integrated pitch/roll control)

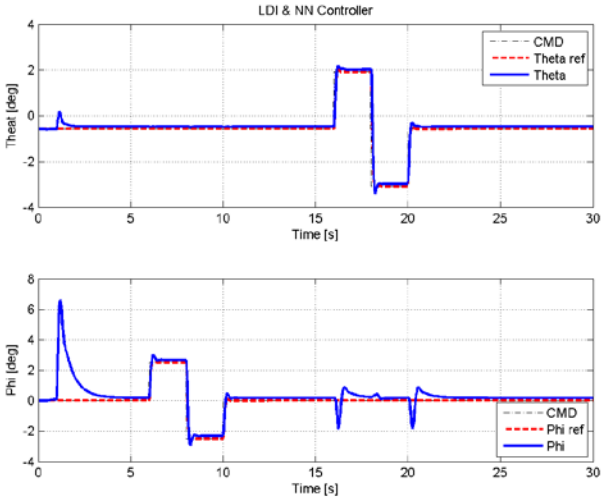

Fig. 14 Responses of state (Top: Pitch angle, Bottom: Roll angle)

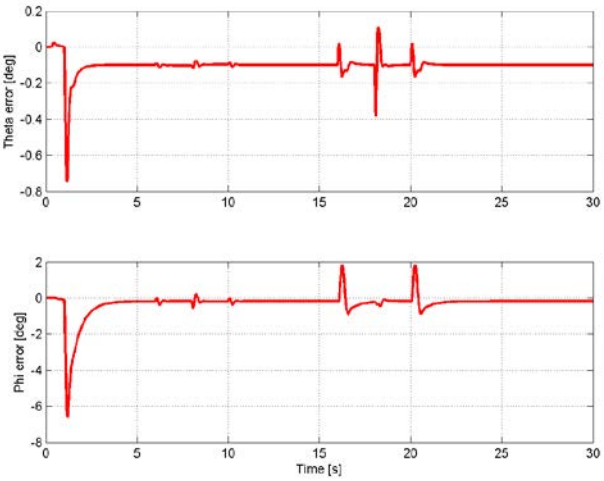

Fig. 15 Attitude error (Top: Pitch angle, Bottom: Roll angle)

Figure 14 shows the similar trends to Figure 10. However, pitch axis error and pitch axis output layer gain are remarkably larger than Case 1.

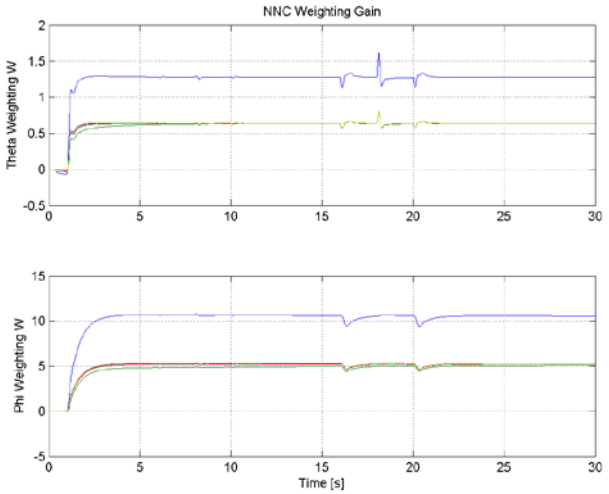

Fig. 16 NN adaptation weight W (Top: Pitch angle, Bottom: Roll angle)

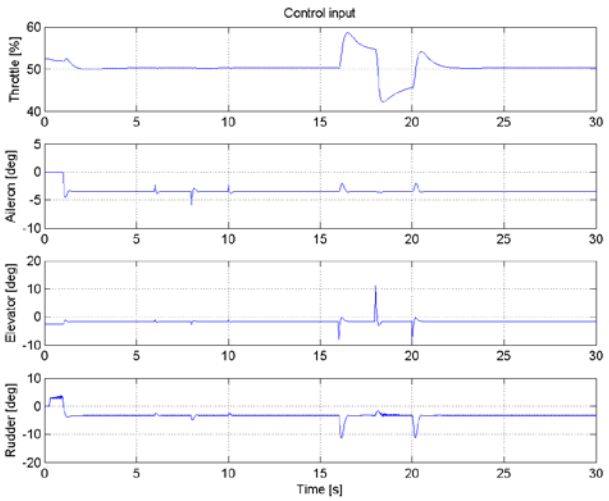

Fig. 17 Responses of throttle and control surfaces

4.3 Result analysis

Table 2 shows the state error norm and output layer weight gain norm in no damage condition simulation. Both results indicate a very similar performance.

Table 2 Comparison of no damage condition simulation

		Case1	vs	Case2
State error	Theta	1.3906	≈	1.3474
	Phi	1.6073	≈	1.6069
Weight W	Theta	7.6265	>	6.0975
	Phi	20.5134	≈	20.5162

Table 3 shows the state error norm and output layer weight gain norm in complex damage condition simulation. Case1 show the good performance compared to case2.

Table 3 Comparison of complex damage condition simulation

		Case1	vs	Case2
State error	Theta	1.9901	<	4.4750
	Phi	29.6758	≈	29.3705
Weight W	Theta	24.6152	<	72.5667
	Phi	588.0752	≈	588.1356

5 Conclusions

This paper considered a complex damage with partial wing and vertical tail loss of blended-wing-body type UAV. Neural network adaptive controller was designed for the UAV. Also, the response of the damaged UAV has been investigated through numerical simulation. This research identified the neural network control system to remove the instability caused by the complex damage.

And, two kinds of inverse controllers has been applied. First inversion controller is designed to separate the roll and pitch axis. But, second case is designed to fuse the roll and pitch axis.

Each inversion controller shows a similar performance at no damaged normal simulation. However, each controller represents a different performance at the complex damage simulation. Case1 inversion controller represents the better performance than Case2. Because in damage situation, the roll axis uncertainty badly influences the pitch axis. So if the damage condition is predicted, it is recommended to design each axis controller separately.

References

[1] Page A, Meloney E, and Monaco J. Flight Testing of a Retrofit Reconfigurable Control Law Architecture Using an F/A-18C, *AIAA Guidance, Navigation and Control Conference*, Keystone, CO, Aug. 21-24, 2006.

[2] Jourdan D, Piedmonte M, Gavrilets V, Vos D, and McCormick J. Enhancing UAV Survivability Through Damage Tolerant Control, *AIAA Guidance, Navigation, and Control Conference*, Toronto, Ontario Canada, Aug. 2-5, 2010.

[3] Dydek Z, Annaswamy A, and Lavretsky E. Adaptive Control of Quadrotor UAVs : A Design Trade Study With Flight Evaluations. *IEEE Transactions on Control Systems Technology*, Vol. 21, No. 4, pp 1400-1406, 2013.

[4] Chowdhary G, Johnson E, Chandramohan R, Kimbrell M, and Calise A. Guidance and Control of Airplanes Under Actuator Failures and Severe Structural Damage, *Journal of Guidance, Control, and Dynamics*, Vol. 36, No. 4, pp 1093-1104, 2013.

[5] Kim K, Ahn J, Kim S, Choi J, Suk J, Lim H, and Hur G. Analysis of partial wing damage on flying-wing unmanned air vehicle. *Proceedings of the Institution of Mechanical Engineers, Part G: Journal of Aerospace Engineering*, Vol. 228, No. 3, pp 355-374, 2014.

[6] Calise A, Lee S, and Sharma M. Development of a Reconfigurable Flight Control Law for Tailless Aircraft. *Journal of Guidance, Control and Dynamics*, Vol.24, No.5, pp 896-902, 2001.

Contact Author Email Address

- Kijoon Kim (mailto : kjoon2008@gmail.com)
- Jongmin Ahn (mailto:ajmkja@add.re.kr)
- Seungkeun Kim (mailto: skim78@cnu.ac.kr)
- Jinyoung Suk (corresponding author, mailto : jsuk@cnu.ac.kr)

Copyright Statement